Quantification of Acetabular Coverage on 3-Dimensional Reconstructed Computed Tomography Scan Bone Models in Patients With Femoroacetabular Impingement Syndrome

A Descriptive Study

Steven F. DeFroda,* MD, Thomas D. Alter,*† MS, Floor Lambers,‡ PhD, Philip Malloy,*§ PhD, Ian M. Clapp,* MD, Jorge Chahla,* MD, PhD, and Shane J. Nho,* MD, MS

Investigation performed at Rush University Medical Center, Chicago, Illinois, USA

Background: Accurate assessment of osseous morphology is imperative in the evaluation of patients with femoroacetabular impingement syndrome (FAIS) and hip dysplasia. Through use of computed tomography (CT), 3-dimensional (3D) reconstructed hip models may provide a more precise measurement for overcoverage and undercoverage and aid in the interpretation of 2-dimensional radiographs obtained in the clinical setting.

Purpose: To describe new measures of acetabular coverage based on 3D-reconstructed CT scan bone models.

Study Design: Cross-sectional study; Level of evidence, 3.

Methods: Preoperative CT scans were acquired on the bilateral hips and pelvises of 30 patients before arthroscopic surgical intervention for FAIS. Custom software was used for semiautomated segmentation to generate 3D osseous models of the femur and acetabulum that were aligned to a standard coordinate system. This software calculated percentage of total acetabular coverage, which was defined as the surface area projected onto the superior aspect of the femoral head. The percentage of coverage was also quantified regionally in the anteromedial, anterolateral, posteromedial, and posterolateral quadrants of the femoral head. The acetabular clockface was established by defining 6 o'clock as the inferior aspect of the acetabular notch. Radial coverage was then calculated along the clockface from the 9-o'clock to 5-o'clock positions.

Results: The study included 20 female and 10 male patients with a mean age of 33.6 ± 11.7 years and mean body mass index of 27.8 ± 6.3. The average percentage of total acetabular coverage for the sample was 57% ± 6%. Acetabular coverages by region were as follows: anteromedial, 78% ± 7%; anterolateral, 18% ± 7%, posterolateral, 33% ± 13%, and posteromedial, 99% ± 1%. The acetabular coverage ranged from 23% to 69% along the radial clockface from 9 to 5 o'clock.

Conclusion: This study demonstrated new 3D measurements to characterize acetabular coverage in patients with FAIS and elucidated the distribution of acetabular coverage according to these measurements.

Keywords: hip arthroscopy; femoroacetabular impingement; hip dysplasia; pincer; acetabular coverage

Acetabular coverage is an important component in the evaluation of hip dysplasia and femoroacetabular impingement (FAI) syndrome (FAIS). Acetabular coverage has been traditionally based on anteroposterior (AP) and lateral radiographs by calculating the intersected area of the femoral head (represented as a circle) with the anterior and/or posterior acetabular walls.[11,24] The lateral center-edge angle (LCEA) is one of the more commonly utilized measurements in the assessment of acetabular under- or overcoverage. The LCEA was originally described in 1940 by Wiberg and was used as a measure of acetabular development and degree of displacement of the femoral head.[26] Although more recent methods have accounted for pelvic tilt, the LCEA is traditionally determined by the angle between a vertical reference line bisecting the center of the femoral head and a second line from the center of the femoral head

The Orthopaedic Journal of Sports Medicine, 9(11), 23259671211049457
DOI: 10.1177/23259671211049457
© The Author(s) 2021

This open-access article is published and distributed under the Creative Commons Attribution - NonCommercial - No Derivatives License (https://creativecommons.org/licenses/by-nc-nd/4.0/), which permits the noncommercial use, distribution, and reproduction of the article in any medium, provided the original author and source are credited. You may not alter, transform, or build upon this article without the permission of the Author(s). For article reuse guidelines, please visit SAGE's website at http://www.sagepub.com/journals-permissions.

to the lateral aspect of the acetabular rim. Wiberg originally defined values of 25° to 40° as normal in adults; values of 20° to 25° as indeterminate; angles <20° as dysplastic; and measurements >40° as representing overcoverage, such as in pincer-type FAI.[11,24] This measurement was originally obtained and validated on 2-dimensional (2D) images, specifically, AP radiographs.[10,18]

Given that FAI is a 3-dimensional (3D) phenomenon, additional radiographic views have been incorporated in the evaluation of acetabular rim morphology. Another commonly utilized radiographic parameter for anterior acetabular coverage is the anterior center-edge angle (ACEA). The ACEA is similar to the LCEA; however, it is obtained on a false-profile view. The false-profile view is obtained with the foot of the symptomatic hip planted parallel to the radiographic cassette and the pelvis rotated approximately 65° in relationship to the cassette, placing the hip in an externally rotated position.[6] The ACEA is similarly obtained using 2 lines originating at the center of the femoral head, with 1 extending superior perpendicular to the transverse axis of the pelvis and the other passing through the lateral edge of the acetabulum.[25] Similar criteria are used in the assessment of over- or undercoverage for the LCEA. The LCEA is best for 2D assessment of superolateral coverage of the femoral head, while the ACEA better estimates anterior coverage.[3] The definition of these angles was further refined by Ogata et al,[20] who described the effect of acetabular retroversion on these measurements. Those authors reported that using the lateral edge of the acetabulum overestimates the functional coverage and proposed redefining the lateral limit of the LCEA and the ACEA as the most superolateral point of the sclerotic weightbearing portion of the acetabulum.[20] This gives a more functional assessment of coverage. The traditional Wiberg method has been found to overestimate coverage by 4° on average by including an area of acetabulum that is posterior to the true 12-o'clock position and does not contribute to osseous contact with the femoral head.[12]

These discrepancies on 2D images have led to investigations utilizing more advanced 3D assessment of acetabular coverage as imaging techniques have improved. Monazzam et al[18] validated the usage of computed tomography (CT) in the measurement of LCEA. By studying CT scans in 22 patients, the authors found high inter- and intraobserver reliability when using CT scans to calculate LCEA.[18] Attempts have also been made at utilizing 3D models to evaluate acetabular coverage. Wylie et al[29] expanded on previous work comparing the traditional LCEA (of Wiberg) and modified sourcil LCEA by examining the sagittal clock-face location of the 2 angles. Those authors showed that the sourcil-edge LCEA represents anterosuperior coverage while the bone-edge LCEA of Wiberg more accurately defines superolateral coverage.[29] This is important during preoperative planning in best understanding where patients have deficient or excessive acetabular coverage. Three-dimensional methods of assessing acetabular coverage often calculate the percentage area covered after projection on a best-fit sphere[11,16] or projection onto a circle on a transverse plane.[9]

The purpose of our study was to demonstrate new measures of acetabular coverage generated from 3D-reconstructed CT models. We hypothesized that the radial acetabular coverage would be greatest between 11 o'clock and 1 o'clock and that measures based on 2D models of acetabular coverage would correlate with 3D measures of coverage.

METHODS

Patient Selection and Imaging

After institutional review board approval, patients meeting the study inclusion criteria were prospectively recruited. All participants provided written and informed consent. The study included patients undergoing primary hip arthroscopy with clinical and radiographic evidence of FAIS. The senior author (S.J.N.) evaluated and diagnosed all participants with FAIS based on radiographic evidence of cam (alpha angle, >50°)[2,15,19] or pincer morphology (LCEA, >40°; positive crossover sign; or acetabular index, <0°),[21] failure of nonoperative management (oral nonsteroidal anti-inflammatory drugs and/or intra-articular cortisone injection, physical therapy), hip pain for >3 months, and a positive anterior impingement sign on examination. Excluded were patients undergoing revision hip arthroscopy, patients with developmental hip disorders (Legg-Calvé-Perthes disease, slipped capital femoral epiphysis), and patients with CT imaging from an outside facility.

Preoperative CT scans of 30 patients undergoing primary hip arthroscopy for FAIS were acquired. CT imaging included 2 regions of interest: both left and right hips from

†Address correspondence to Thomas D. Alter, MS, Department of Orthopaedic Surgery, Rush University Medical Center, Chicago, IL 60010, USA (email: nho.research@rushortho.com).

*Section of Young Adult Hip Surgery, Division of Sports Medicine, Department of Orthopaedic Surgery, Hip Preservation Center, Rush University Medical Center, Chicago, Illinois, USA.

‡Stryker Sports Medicine, Kalamazoo, Michigan, USA.

§Arcadia University, Montgomery, Pennsylvania, USA.

Final revision submitted July 6, 2021; accepted July 19, 2021.

One or more of the authors has declared the following potential conflict of interest or source of funding: S.F.D. has received education payments from Medical Device Business Services and hospitality payments from Zimmer Biomet. F.L. is an employee of Stryker. J.C. has received education payments from Arthrex and Smith & Nephew; consulting fees from Arthrex, DePuy, Linvatec, Ossur, and Smith & Nephew; nonconsulting fees from Linvatec; and hospitality payments from Medwest Associates and Stryker. S.J.N. has received research support from Allosource, Arthrex, Athletico, DJO, Linvatec, Miomed, Smith & Nephew, and Stryker; education payments from Elite Orthopedics; consulting fees from Ossur and Stryker; and royalties from Ossur, Stryker, and Springer. AOSSM checks author disclosures against the Open Payments Database (OPD). AOSSM has not conducted an independent investigation on the OPD and disclaims any liability or responsibility relating thereto.

Ethical approval for this study was obtained from Rush University Medical Center (ORA No. 12022108-IRB01-CR07).

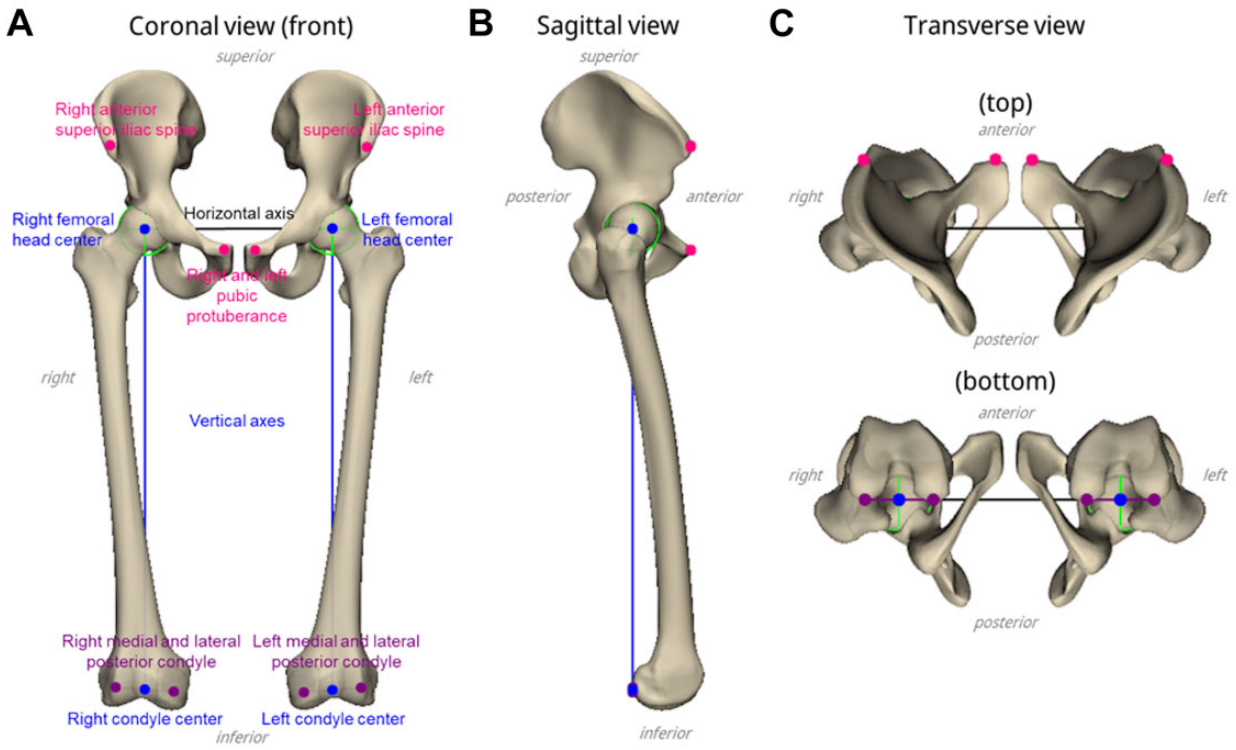

Figure 1. Definition of the anatomical planes. (A) The pelvic coronal plane was defined by the left and right anterior superior iliac spine and pubic protuberance (red dots). The pelvic transverse plane was perpendicular to the coronal plane and in line with the horizontal axis (black line), defined by the left and right femoral head centers (blue dots). The pelvic sagittal plane was perpendicular to the coronal and transverse planes. The femoral coronal plane was defined by the femoral head center and the medial and lateral posterior condyles (purple dots). (B) The femoral sagittal plane was perpendicular to the coronal plane and in line with the vertical axis (blue line), defined by the femoral head center and posterior condylar center (blue dots). (C) The femoral transverse plane was perpendicular to the coronal plane and sagittal planes.

the anterior superior iliac spine to below the lesser trochanter as well as the knee. It was ensured that there was no motion or other image artifacts and that the scans were acquired in the same frame of reference to ensure that the spatial relationship between the pelvis/proximal femur and knee scan was known. Excluded were patients with prior ipsilateral hip surgery. The CT scanner (BrightSpeed; GE Healthcare) used the following acquisition parameters: 120 kV, 250 mAs, slice thickness of 0.675 mm, 512 × 512 acquisition matrix, and in-plane resolution of at most 1 × 1 mm. All CT images were exported as Digital Imaging and Communication in Medicine files and stored in our institutional picture archiving and communication system.

3D Geometric Modeling of Preoperative CT Scans

We created 3D models of the left and right proximal femur, pelvis, and distal femur (knee) using semiautomated segmentation. Segmentation of both femurs was required to make acetabular measurements, yet measurements were only performed on the operative extremity. The initial segmentation was based on a statistical shape model and random forest optimization. Statistical shape models have been established as a robust tool for segmentation of medical images.[13] Random forest optimization can further improve the accuracy of the automated segmentation.[1,8] The segmentation was reviewed and manually edited if necessary by trained operators and personnel with doctoral degrees in image processing (F.L.). A custom software (Stryker Corp) was used to align the models according to a standard coordinate system and to generate the 3D osseous models. Alignment of the 3D models was performed to reduce the effect of inaccuracies caused by differences in patient positioning during image acquisition.[22,23] The 3D models were aligned by rotating around the femoral head center (of the treatment side). In order to align the 3D models, anatomic planes were defined by morphological landmarks (Figure 1). For the pelvis, the coronal plane was defined by the anterior pelvic plane (left and right anterior superior iliac spines and left and right pubic protuberances) and the horizontal axis by left and right femoral head centers. The femoral head centers were defined by a best-fit sphere to the loadbearing surface of the femoral head. For the femur, the line from the femoral head center to the center of the posterior condyles was equivalent to the vertical axis (perpendicular to the transverse plane of the pelvis), and the posterior condylar axis was equivalent to the coronal plane.

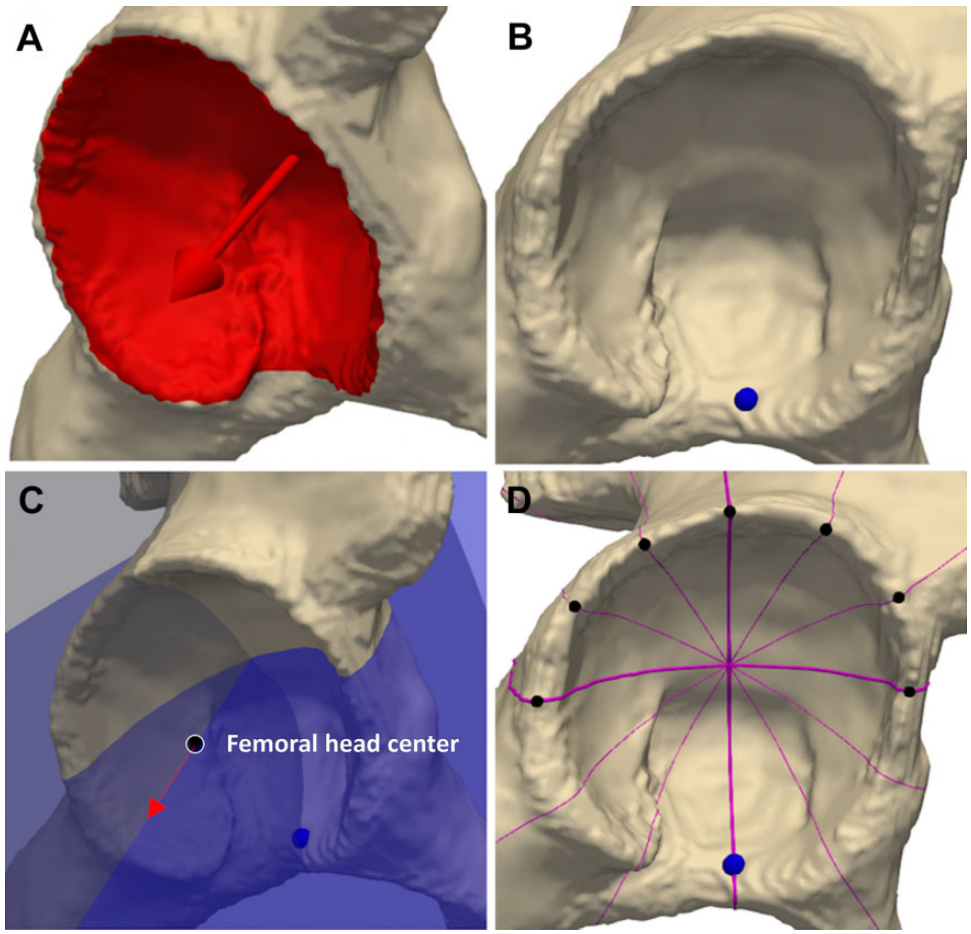

Figure 2. The (A) normal line of the acetabular cup (arrow), (B) midpoint of the traverse ligament at the inferior acetabular notch (blue dot), and (C) femoral head center (black dot) were used to define the acetabular clockface location. (D) The points on the clockface were defined by rotating planes around the normal line of the acetabular cup surface.

Defining the Acetabular Clockface

The location of the acetabular clockface was defined by the acetabular cup geometric normal line, and the transverse ligament midpoint at the inferior acetabular notch. With the midpoint of the transverse ligament center as the 6-o'clock reference point, the points on the clockface were defined by rotating planes around the normal line of the acetabular cup surface (Figure 2). The 12-o'clock and 3-o'clock positions were superior and anterior, respectively.

Measurements Based on 3D Models

On 3D-reconstructed CT models, the LCEA was calculated as the angle between the sagittal plane and the line from the center of the femoral head to the acetabular rim point at the 12-o'clock position (Figure 3). The Tönnis angle (acetabular inclination) was based on an angle between 2 lines originating at the point at which the lunate surface and acetabular fossa met. The first line was based on the transverse plane, while the second line was directed toward the superior aspect of the lunate surface at the 12-o'clock position (Figure 4).

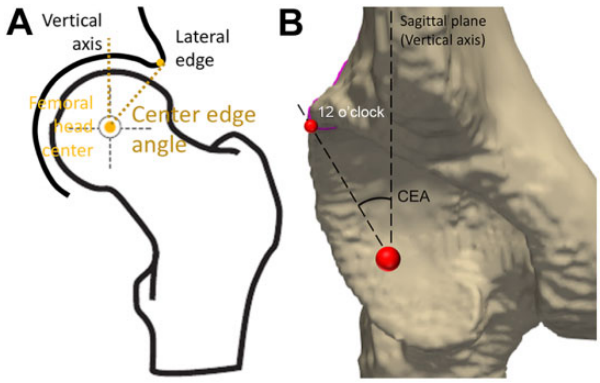

Figure 3. (A) Schematic depiction and (B) measurement of the lateral center-edge angle on a 3D-reconstructed CT model, determined by the angle between the sagittal plane and the line from the center of the femoral head center (large red sphere) to the acetabular rim point at the 12-o'clock position (small red sphere). CEA, center-edge angle. The yellow dots correspond to the center of the femoral head and the lateral edge of the acetabulum at the 12-o'clock position.

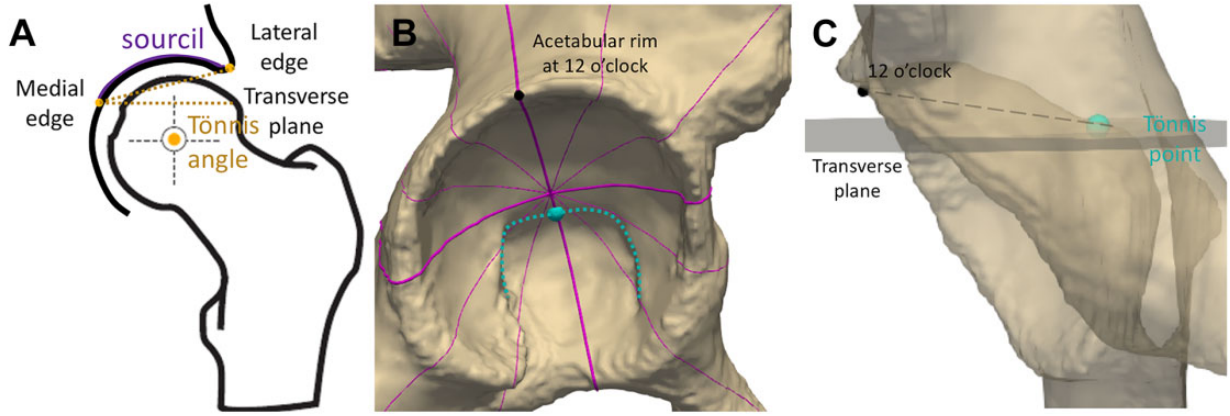

Figure 4. (A) Schematic depiction of the Tönnis angle measure. (B) The transition from the lunate surface to the acetabular fossa was identified (green dotted line), and the 12-o'clock point of the transition (green sphere) was identified. (C) Measurement of the Tönnis angle on a 3D-reconstructed CT model was based on the angle between 2 lines originating at the point. The first line was based on the transverse plane, while the second line (dashed line) was directed toward the superior aspect of the lunate surface at the 12-o'clock position.

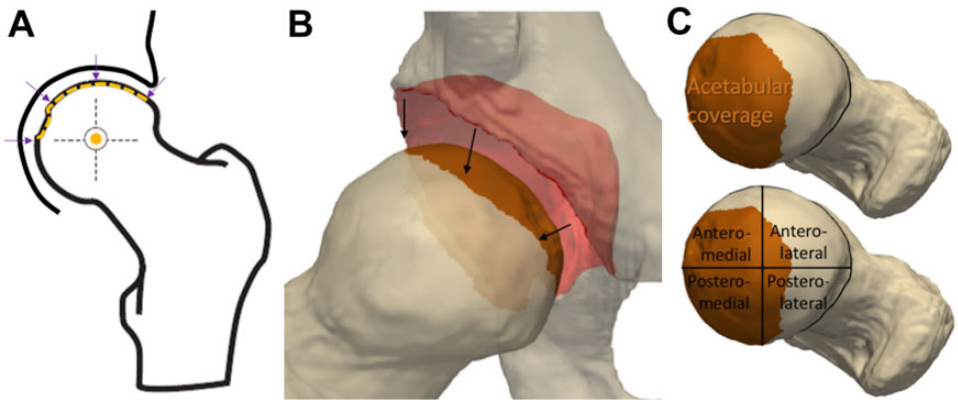

Figure 5. (A) Schematic depiction and (B) representation on a 3D-reconstructed CT model of acetabular coverage of the femoral head measured as (C) total acetabular coverage. The arrows indicate the region of the femoral head that is covered by the acetabulum.

Acetabular coverage was defined as the percentage surface area of the superior half of the femoral head contained within the acetabulum. To calculate total acetabular coverage, we drew a curve at the inner apex of the acetabular rim and projected onto the femoral head. The superior half of the femoral head was defined as the surface area above the transverse plane at the femoral head center.

It has been shown that dividing acetabular coverage into quadrants can make the measurement more sensitive.[5] Therefore, acetabular coverage was also calculated in the anteromedial, anterolateral, posteromedial, and posterolateral quadrants. The quadrants were created by intersecting the surface areas with the coronal and sagittal planes at the superior femoral head center (Figure 5).

Radial coverage was calculated at each clockface position from 9 o'clock to 5 o'clock, as these are the positions most relevant to acetabular coverage. Radial coverage was based on the angle between 2 lines as previously described.[16] The first line was the horizontal axis (mediolateral line connecting the left and right femoral head centers). The second line was from the center of the femoral head to the acetabular rim at each clockface. The angle was converted to percentage coverage, with a maximum of 180° or 100% coverage (Figure 6). For both the radial coverage measurement at 12 o'clock and the LCEA, the line between the femoral head center and the acetabular rim at 12 o'clock was used, but the difference between the measurements was that radial coverage was measured as the Euclidean angle between that line and the horizontal axis while for the LCEA it was the projected angle to the coronal plane or equivalent: the angle between that line and the sagittal plane. There was a correlation between LCEA and radial coverage at 12 o'clock. The 3D model–based measurements were calculated using Stryker custom software (Stryker Corp) and 3-matic (Materialise). The Stryker custom software has been validated according to internal design control

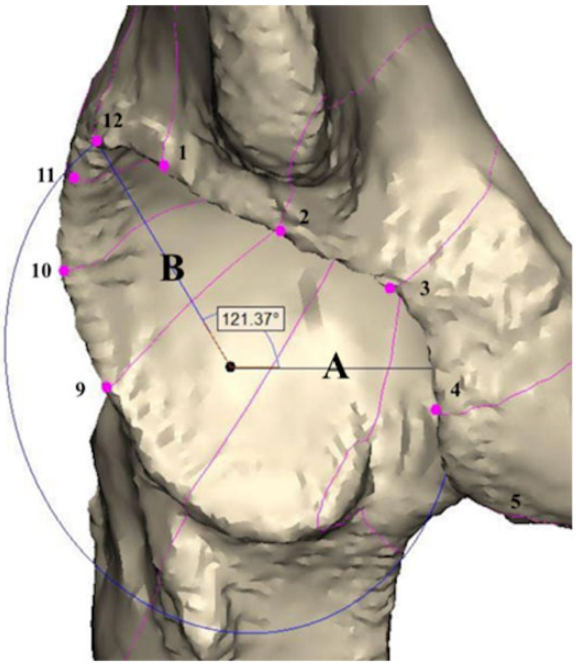

Figure 6. The 3D model–based measure of radial coverage was determined based on the angle between 2 lines: a line connecting the center of each femoral head (horizontal axis) (*A*) and a separate line connecting the center of the femoral head and the acetabular rim (*B*).

procedures (IEC 62304), and 3-matic is a software validated for medical usage (510(k) No. K060950).

Reliability Analysis

The intraobserver reliabilities (intraclass correlation coefficients [ICCs]) were as follows: LCEA (ICC, 0.98; $P < .001$), Tönnis angle (ICC, 0.84; $P = .011$), and total acetabular coverage (ICC, 0.95; $P = .001$). Based on 3 ratings by 3 trained and blinded graders on 3 separate sets of segmented bone models, the interobserver reliabilities for coverage measurements were as follows: LCEA (ICC, 0.96; $P < .001$), Tönnis angle (ICC, 0.88; $P = .007$), and total acetabular coverage (ICC, 0.96; $P < .001$), strong interobserver reliabilty for coverage measures were demonstrated.

Statistical Analysis

The primary dependent variables of interest included model-based 3D measures of coverage and model-based 2D measures of coverage. Model-based 3D measures of coverage included total coverage and quadrant-specific coverage (anteromedial, anterolateral, posteromedial, and posterolateral). Additional measures of coverage included LCEA, Tönnis angle, and radial coverage (percentage). All data were inspected before analysis to determine if parametric statistical analysis assumptions were met. In cases of assumption violation, nonparametric statistical tests were applied. The Shapiro-Wilk test was used to determine normality, and box plots were used to identify outliers. Pearson (r) product-moment or Spearman rank correlation analysis was performed between model-based 3D and model-based 2D measures, with an a priori alpha level of .01 used to define statistical significance. All statistical testing was performed using SPSS Version 26 (IBM Corp).

TABLE 1
Measures for All Variables of Interest[a]

Variable	Mean ± SD
3D model	
Total coverage, %	56.7 ± 5.9
Anteromedial coverage, %	77.5 ± 6.6
Anterolateral coverage, %	17.7 ± 6.7
Posteromedial coverage, %	99.2 ± 1.4
Posterolateral coverage, %	32.8 ± 13.0
2D model	
Lateral center-edge angle, deg	35.4 ± 8.5
Tönnis angle, deg	5.5 ± 6.5

[a]2D, 2-dimensional; 3D, 3-dimensional.

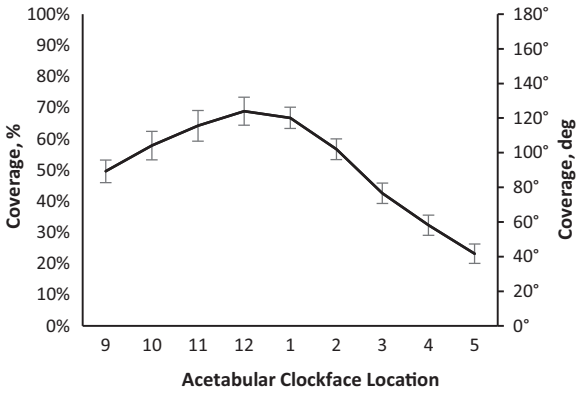

Figure 7. Graph showing 2D radial acetabular coverage by acetabular clockface location. Error bars indicate the standard deviation of radial coverage measures for the entire cohort at each acetabular clock face.

RESULTS

Patient Cohort

The study sample included 20 female and 10 male patients with a mean age of 33.6 ± 11.7 years and mean BMI of 27.8 ± 6.3. The mean coverage for the cohort was 56.7% ± 5.9% (Table 1). Analysis of radial coverage from the 9-o'clock to 5-o'clock positions indicated that the greatest radial coverage was located at the 12-o'clock position (Figure 7).

Model-Based 3D and 2D Measures

Spearman correlation analyses indicated significant bivariate correlations between 3D measures of total acetabular coverage and model-based measures of LCEA and Tönnis

TABLE 2
Correlation Coefficient (r) Between 3D and 2D Measures of Acetabular Coverage on 3D Models[a]

	Total	Anteromedial	Anterolateral	Posteromedial	Posterolateral
LCEA	**0.859**	**0.578**	**0.730**	0.386	**0.829**
Tönnis angle	**–0.588**	**–0.513**	**–0.609**	–0.036	**–0.462**

[a]Bold values indicate statistical significance ($P < .01$). 2D, 2-dimensional; 3D, 3-dimensional; LCEA, lateral center-edge angle.

angle (Table 2). In addition, acetabular coverage by quadrant had significant correlation with the LCEA and Tönnis angle (Table 2).

DISCUSSION

Using CT scan imaging and new 3D image–based modeling measures, we were able to produce an average distribution of acetabular coverage in patients with FAIS. In our cohort, the average total acetabular coverage was 56.7%, the greatest radial coverage occurred at 12 o'clock, and the posterolateral quadrant coverage demonstrated the greatest variability and correlated strongest with the LCEA on 2D modeling. FAI is a 3D condition that is typically evaluated via 2D imaging techniques and measurements. However, studies have shown that these measurements have varying degrees of accuracy based on both image quality and operator interpretation.[12,18,29] Misinterpretation or misunderstanding of measuring acetabular coverage via the LCEA can lead to incorrect assessment of acetabular morphology, which may also lead to under- or overresection during hip arthroscopy.[29] By generating a 3D imaging study before surgical intervention, the surgeon can have a patient-specific representation of the patient's bony anatomy in the clinic and operating room.

The present study found that the greatest radial acetabular coverage was at 12 o'clock. This is important because the 12-o'clock position typically corresponds to the lateral aspect of the acetabulum measured via the traditional bone-edge LCEA measurement.[12,29] Specifically, Wylie et al[29] found that performing sourcil LCEA measurement caused the LCEA to measure at the 12:50 position, compared with 12:00 for the bone-edge LCEA. This is an important distinction when determining preoperative LCEA by understanding that the sourcil-based LCEA represents more anterosuperior coverage compared with the bone-edge LCEA, which represents superior and lateral coverage.[29] The 3D measures of radial acetabular coverage may limit these discrepancies and may better guide rim resection at the time of surgery.

This can be a beneficial tool for both less and more experienced hip surgeons alike by allowing them to better understand the complex anatomy in FAIS, specifically in patients with acetabular version and coverage abnormalities. Ogata et al[20] reported that the use of the traditional bone-edge LCEA measurement yields an overestimate of the functional lateral coverage in patients with acetabular retroversion and hip dysplasia. A better understanding of 3D morphology can help surgeons avoid overresection when performing acetabuloplasty and potentially destabilizing the hip joint. In addition, there remains debate and ongoing investigation as to the effect of varying degrees of acetabular resection when performing acetauloplasty. Johannsen et al[14] reported their 5-year postoperative outcomes in patients classified via postoperative LCEA as dysplastic (<20°), borderline dysplastic (20°-25°), normal (25°-35°), and borderline overcovered (>35°). Patients were also classified by acetabular resection depth ranging from 5° to 10° differences from pre- to postoperative LCEA. Johannsen et al found no statistically significant differences in patients with abnormal LCEA or by degrees of resection, indicating that even patients who required large resections did well at midterm follow-up. This further emphasizes the importance of understanding the 3D anatomy of the acetabulum, as patients will require varying amounts of rim resection based on morphology.

Our model also found that the 3D LCEA correlated strongest with posterolateral coverage. Considering that a majority of resection will occur laterally, this is the crucial area in assessing acetabular geometry. By providing the surgeon with a better understanding of the 3D anatomy of the acetabulum and its relationship to femoral head coverage, a proper resection can be assessed in real time. Additionally, by generating a 3D model of acetabular coverage, the surgeon can avoid error associated with relying on static 2D images, whether on radiographs or CT scans. It has been shown that when assessing CT scans of the midsagittal plane of the femur, the LCEA measurements are greater than those measured on plain radiographs alone.[18] Chadayammuri et al[4] found that CT scan values were on average 2.1° greater than those on plain films, with subgroup analysis finding that patients with concomitant acetabular dysplasia and cam-type FAI had a mean difference of 5.5°. This variation underplays the importance of a consistent modeling technique when evaluating patients before surgery, as a difference of 5° could be the difference between an arthroscopic procedure and a pelvic-acetabular osteotomy. By producing a 3D model of the hip, the surgeon can better understand various morphologies and relate it to the 2D image that is readily available in the operating room.[27]

While femur-sided impingement was not evaluated in this study, it has previously been demonstrated that femur-sided cam lesions are a major contributor to FAIS, with insufficient resection being a major cause of revision hip arthroscopy.[7] Milone et al[17] utilized CT scans to define the 3D morphology of cam lesions in 100 patients

requiring hip arthroscopy. With regard to cam impingement, they reported a mean maximum alpha angle of 70.8° at 1:23 and identified 60% of maximum alpha angles between the 12:45 and 1:45 positions. They also noted that 3D CT models located the maximum alpha angle measurements more anterosuperior than did 2D CT and plain radiograph measurements. It is important to consider FAIS a bipolar situation in which there is a complex interplay between acetabular coverage, which our study found to be greatest closer to the 12-o'clock radial position and in the posterolateral quadrant of the femoral head, and femoral cam lesions, which have been reported to be most significant in the anterosuperior femoral neck and often extending laterally.[17]

Limitations

This study is not without limitations. First, we had a relatively small sample size of 30 hips, which could potentially result in selection bias. To reduce potential biases, consecutive patients undergoing surgical management for FAI were included in this study. Second, we did not have a control population of patients without hip pain and therefore were unable to evaluate the amount of bone that needs to be resected to restore normal acetabular coverage. Third, this study focused on image-based characterization of the acetabulum and did not seek to evaluate the relationship between our 3D modeling and conventional radiographic measures of coverage, patient-reported outcomes, associated pathology, or chosen surgical intervention. Fourth, although CT imaging is the clinical "gold standard" for evaluation of the osseous morphology of the hip, it is not without limitations. The use of CT imaging is controversial for the evaluation of FAI in young patients, given the ionizing radiation exposure.[28] However, prior studies have demonstrated absolute agreement between 3D femoral models generated via 1.5-T magnetic resonance imaging and CT imaging. Therefore, our findings should be applicable to both magnetic resonance imaging-based and CT-based bone models. Fifth, while CT imaging captures the osseous components of acetabular coverage, it fails to account for the soft tissue components. Last, femoral morphology was not evaluated in the present study. Despite the limitations of this study, we believe it demonstrated the benefits of 3D modeling of the hip and how it relates to more readily available 2D imaging techniques.

CONCLUSION

In this study, we described novel 3D measurements to characterize acetabular coverage in patients with FAIS and elucidated the distribution of acetabular coverage according to these measurements.

REFERENCES

1. Ambellan F, Tack A, Ehlke M, Zachow S. Automated segmentation of knee bone and cartilage combining statistical shape knowledge and convolutional neural networks: data from the Osteoarthritis Initiative. *Med Image Anal*. 2019;52:109-118.
2. Beaule PE, Zaragoza E, Motamedi K, Copelan N, Dorey FJ. Three-dimensional computed tomography of the hip in the assessment of femoroacetabular impingement. *J Orthop Res*. 2005;23(6):1286-1292.
3. Beck M, Kalhor M, Leunig M, Ganz R. Hip morphology influences the pattern of damage to the acetabular cartilage: femoroacetabular impingement as a cause of early osteoarthritis of the hip. *J Bone Joint Surg Br*. 2005;87(7):1012-1018.
4. Chadayammuri V, Garabekyan T, Jesse MK, et al. Measurement of lateral acetabular coverage: a comparison between CT and plain radiography. *J Hip Preserv Surg*. 2015;2(4):392-400.
5. Cheng H, Liu L, Yu W, et al. Comparison of 2.5D and 3D quantification of femoral head coverage in normal control subjects and patients with hip dysplasia. *PLoS One*. 2015;10(11):e0143498.
6. Clohisy JC, Carlisle JC, Beaulé PE, et al. A systematic approach to the plain radiographic evaluation of the young adult hip. *J Bone Joint Surg Am*. 2008;90(suppl 4):47-66.
7. Cvetanovich GL, Harris JD, Erickson BJ, et al. Revision hip arthroscopy: a systematic review of diagnoses, operative findings, and outcomes. *Arthroscopy*. 2015;31(7):1382-1390.
8. Damopoulos D, Lerch TD, Schmaranzer F, et al. Segmentation of the proximal femur in radial MR scans using a random forest classifier and deformable model registration. *Int J Comput Assist Radiol Surg*. 2019;14(3):545-561.
9. Dandachli W, Kannan V, Richards R, et al. Analysis of cover of the femoral head in normal and dysplastic hips: new CT-based technique. *J Bone Joint Surg Br*. 2008;90(11):1428-1434.
10. Fredensborg N. The results of early treatment of typical congenital dislocation of the hip in Malmo. *J Bone Joint Surg Br*. 1976;58(3):272-278.
11. Fritz B, Agten CA, Boldt FK, et al. Acetabular coverage differs between standing and supine positions: model-based assessment of low-dose biplanar radiographs and comparison with CT. *Eur Radiol*. 2019;29(10):5691-5699.
12. Hanson JA, Kapron AL, Swenson KM, et al. Discrepancies in measuring acetabular coverage: revisiting the anterior and lateral center edge angles. *J Hip Preserv Surg*. 2015;2(3):280-286.
13. Heimann T, Meinzer HP. Statistical shape models for 3D medical image segmentation: a review. *Med Image Anal*. 2009;13(4):543-563.
14. Johannsen AM, Ruzbarsky JJ, Pierpoint LA, et al. No correlation between depth of acetabuloplasty or postoperative lateral center-edge angle on midterm outcomes of hip arthroscopy with acetabuloplasty and labral repair. *Am J Sports Med*. 2021;49(1):49-54.
15. Johnston TL, Schenker ML, Briggs KK, Philippon MJ. Relationship between offset angle alpha and hip chondral injury in femoroacetabular impingement. *Arthroscopy*. 2008;24(6):669-675.
16. Larson CM, Moreau-Gaudry A, Kelly BT, et al. Are normal hips being labeled as pathologic? A CT-based method for defining normal acetabular coverage. *Clin Orthop Relat Res*. 2015;473(4):1247-1254.
17. Milone MT, Bedi A, Poultsides L, et al. Novel CT-based three-dimensional software improves the characterization of cam morphology. *Clin Orthop Relat Res*. 2013;471(8):2484-2491.
18. Monazzam S, Bomar JD, Cidambi K, Kruk P, Hosalkar H. Lateral center-edge angle on conventional radiography and computed tomography. *Clin Orthop Relat Res*. 2013;471(7):2233-2237.
19. Nepple JJ, Brophy RH, Matava MJ, Wright RW, Clohisy JC. Radiographic findings of femoroacetabular impingement in National Football League Combine athletes undergoing radiographs for previous hip or groin pain. *Arthroscopy*. 2012;28(10):1396-1403.
20. Ogata S, Moriya H, Tsuchiya K, et al. Acetabular cover in congenital dislocation of the hip. *J Bone Joint Surg Br*. 1990;72(2):190-196.
21. Rhee C, Le Francois T, Byrd JWT, Glazebrook M, Wong I. Radiographic diagnosis of pincer-type femoroacetabular impingement: a systematic review. *Orthop J Sports Med*. 2017;5(5):2325967117708307.

22. Ross JR, Bedi A, Stone RM, et al. Intraoperative fluoroscopic imaging to treat cam deformities: correlation with 3-dimensional computed tomography. *Am J Sports Med*. 2014;42(6):1370-1376.
23. Ross JR, Nepple JJ, Philippon MJ, et al. Effect of changes in pelvic tilt on range of motion to impingement and radiographic parameters of acetabular morphologic characteristics. *Am J Sports Med*. 2014; 42(10):2402-2409.
24. Tannast M, Fritsch S, Zheng G, Siebenrock KA, Steppacher SD. Which radiographic hip parameters do not have to be corrected for pelvic rotation and tilt? *Clin Orthop Relat Res*. 2015;473(4):1255-1266.
25. Welton KL, Jesse MK, Kraeutler MJ, Garabekyan T, Mei-Dan O. The anteroposterior pelvic radiograph: acetabular and femoral measurements and relation to hip pathologies. *J Bone Joint Surg Am*. 2018; 100(1):76-85.
26. Wiberg G. Studies on dysplastic acetabula and congenital subluxation of the hip joint with special reference to the complication of osteoarthritis. *JAMA*. 1940;115(1):81.
27. Wong TT, Lynch TS, Popkin CA, Kazam JK. Preoperative use of a 3D printed model for femoroacetabular impingement surgery and its effect on planned osteoplasty. *AJR Am J Roentgenol*. 2018;211(2): W116-W121.
28. Wylie JD, Jenkins PA, Beckmann JT, et al. Computed tomography scans in patients with young adult hip pain carry a lifetime risk of malignancy. *Arthroscopy*. 2018;34(1):155-163.e153.
29. Wylie JD, Kapron AL, Peters CL, Aoki SK, Maak TG. Relationship between the lateral center-edge angle and 3-dimensional acetabular coverage. *Orthop J Sports Med*. 2017;5(4):232596 7117700589.